

# The G-Band Systematics of Vibrational and Transitional Nuclei with $A = 150$ to $166$

M. I. El-Zaiki and H. E. Abdel-Baeth

Physics Department, Faculty of Science, Benha 13518, Egypt

Z. Naturforsch. **49a**, 802–810 (1994); received June 7, 1994

The vibrational and rotational characteristics of the ground bands of even-even nuclei with  $150 \leq A \leq 166$  ( $2 < R_4 < 3$ ) are studied. The spectra of these nuclei (with band crossing angular momentum  $I_c \geq 12$ ) are analyzed with a cubic polynomial in  $I$ . The considered nuclei ( $^{150}\text{Sm}$ ,  $^{152}\text{Gd}$ ,  $^{154-156}\text{Dy}$ ,  $^{156}\text{Er}$ ,  $^{158, 160, 162}\text{Yb}$  and  $^{162, 164, 166}\text{Hf}$ ) lie in the central region between the  $Z = 50$  and  $Z = 82$  major shell closures and span the spherical to the well deformed region. The gradual shape transition from a soft spherical vibrator to a deformed rotor from  $^{150}\text{Sm}$  to  $^{166}\text{Hf}$  is thus made explicitly apparent from the g-band spectrum analysis in terms of the vibrational, rotational and softness coefficients.

The transition at  $N = 88-90$  for the vibrational-rotational ratios and for the kinematic moments of inertia are reproduced.

## Introduction

The complex nuclear structure of softly deformed, shape-transitional nuclei with  $N = 88-90-92$  in the  $A = 150 \sim 200$  region has been a challenge to the collective theory [1, 2]. Here, the features of both a spherical vibrator and a deformed rotor are present in the same nucleus. Earlier, Gupta noted [2] that the g-band spectra ( $I \leq 14^+$ ) of  $^{154, 156}\text{Dy}$  are well described by a cubic polynomial in  $I$ .

The applicability of this polynomial is extended, here, to more deformed nuclei. The present work represents an extensive analysis of the g-band structures of the vibrational isotonic chain of  $N = 88$  and the transitional nuclei of  $N = 90, 92$ . Then, the systematics of the g-bands of these nuclei are presented. The vibrational-rotational ratios are reproduced and their variations from, the soft spherical  $^{150}\text{Sm}$  to deformed  $^{166}\text{Hf}$  are discussed.

The question concerning the variation of deformation across a shell, i.e. the gradual shape transition may be empirically answered by examining the systematics of the moments of inertia as a function of spin and position in the shell [3].

## I. The G-Bands Systematics

The ground-band spectra of the investigated nuclei are described by the cubic polynomial [2, 4].

$$E(I) = aI + bI^2 + cI^3 \quad (1)$$

$$= (a-b)I + bI(I+1) + cI^3. \quad (2)$$

The cubic polynomial is used to illustrate the necessity of each of the three terms, the vibrational  $(a-b)I$  term, the rotational  $bI(I+1)$  term and rotation-vibration interaction  $cI^3$  term. In order to find the relative contribution of the vibrational and rotational terms in (2) we have done a least square fitting to the spectra for the g-band states up to  $I^\pi \leq 18^+$  after the crossing.

### 1. G-Bands in $^{150}\text{Sm}$ , $^{152}\text{Gd}$ and $^{156}\text{Er}$

The three nuclei are almost spherical with  $R_4 = E_4/E_2$  values of 2.316, 2.194 and 2.315, respectively. Table I.1 lists the values of the parameters  $a, b, c$ . The vibrational structure of the g-band in each of the three isotones ( $N = 88$ ) is reflected in the much larger value of the parameter  $a$  with  $b/(a-b)$  in (2) at only  $\sim 10.9\%$  ( $^{150}\text{Sm}$ ),  $6.5\%$  ( $^{152}\text{Gd}$ ) and  $15.4\%$  ( $^{156}\text{Er}$ ). The interaction term  $c$  is quite small for each isotone. These values imply only a small rotational component in the  $2_g$  state. In  $^{152}\text{Gd}$  ( $Z = 64$ ),  $(a-b)$  is larger than the other two values for  $^{150}\text{Sm}$  ( $Z = 62$ ),  $^{156}\text{Er}$  ( $Z = 68$ ) and even larger than the corresponding value for  $^{154}\text{Dy}$  ( $Z = 66$ ) (see Table I.2). This indicates that the vibrational contribution in the  $2_g$  state is much larger at the closed shell ( $Z = 64$ ) for these  $N = 88$  isotones.

### 2. G-Bands in $^{154, 156}\text{Dy}$

The proton rich  $^{154, 156}\text{Dy}$  isotopes lie midway between  $Z = 50$  and  $Z = 82$ .  $^{154}\text{Dy}$  is almost spherical

Reprint requests to Prof. M. I. El-Zaiki.

0932-0784 / 94 / 0700-0802 \$ 06.00 © – Verlag der Zeitschrift für Naturforschung, D-72027 Tübingen



Dieses Werk wurde im Jahr 2013 vom Verlag Zeitschrift für Naturforschung in Zusammenarbeit mit der Max-Planck-Gesellschaft zur Förderung der Wissenschaften e.V. digitalisiert und unter folgender Lizenz veröffentlicht: Creative Commons Namensnennung-Keine Bearbeitung 3.0 Deutschland Lizenz.

Zum 01.01.2015 ist eine Anpassung der Lizenzbedingungen (Entfall der Creative Commons Lizenzbedingung „Keine Bearbeitung“) beabsichtigt, um eine Nachnutzung auch im Rahmen zukünftiger wissenschaftlicher Nutzungsformen zu ermöglichen.

This work has been digitalized and published in 2013 by Verlag Zeitschrift für Naturforschung in cooperation with the Max Planck Society for the Advancement of Science under a Creative Commons Attribution-NoDerivs 3.0 Germany License.

On 01.01.2015 it is planned to change the License Conditions (the removal of the Creative Commons License condition "no derivative works"). This is to allow reuse in the area of future scientific usage.

Table I.1. The parameters  $a$ ,  $b$ ,  $c$  of the cubic polynomial (2) for  $^{150}\text{Sm}$ ,  $^{152}\text{Gd}$ ,  $^{156}\text{Er}$  (in keV) for the ground band.

Nu- cleus	$a$	$b$	$c$	$b/a-b$	$E_{\text{vib}}\%$	$E_{\text{rot}}\%$	$E_{\text{rot}}/$ $E_{\text{vib}}$
$^{150}\text{Sm}$	142	14	-0.386	0.109	75	24.9	0.33
$^{152}\text{Gd}$	154.36	9.36	-0.179	0.064	84	16	0.19
$^{156}\text{Er}$	136.70	18.30	-0.590	0.154	69	32	0.46

Table I.2. The parameters  $a$ ,  $b$ ,  $c$  of the cubic polynomial (2) for  $^{154,156}\text{Dy}$  (in keV) for the ground band.

Nu- cleus	$a$	$b$	$c$	$b/a-b$	$E_{\text{vib}}\%$	$E_{\text{rot}}\%$	$E_{\text{rot}}/$ $E_{\text{vib}}$
$^{154}\text{Dy}$	148.84	10.16	-0.196	0.073	82	18	0.22
	149.2*	10.35	-0.220	0.070	—	—	0.21*
$^{156}\text{Dy}$	35.1	17.9	-0.410	1.040	25	77	3.10
	38.7*	17.0	-0.360	0.800	—	—	2.40*

\* Ref. [2]: g-band ( $I \leq 14^+$ ), present work: g-band ( $I \leq 18^+$ ).Table I.3. The parameters  $a$ ,  $b$ ,  $c$  of the cubic polynomial (2) for  $^{158,160,162}\text{Yb}$  (in keV) for the ground band.

Nu- cleus	$a$	$b$	$c$	$b/a-b$	$E_{\text{vib}}\%$	$E_{\text{rot}}\%$	$E_{\text{rot}}/$ $E_{\text{vib}}$
$^{158}\text{Yb}$	144.70	18.17	-0.530	0.144	70.7	30	0.42
$^{160}\text{Yb}$	79.30	23.46	-0.810	0.420	45	57	1.27
$^{162}\text{Yb}$	41.30	22.46	-0.630	1.192	22.5	80	3.56

Table I.4. The parameters  $a$ ,  $b$ ,  $c$  of the cubic polynomial (2) for  $^{162,164,166}\text{Hf}$  (in keV) for the ground band.

Nu- cleus	$a$	$b$	$c$	$b/a-b$	$E_{\text{vib}}\%$	$E_{\text{rot}}\%$	$E_{\text{rot}}/$ $E_{\text{vib}}$
$^{162}\text{Hf}$	101.50	22.97	-0.690	0.292	54	47	0.87
$^{164}\text{Hf}$	59.60	24.50	-0.739	0.698	33	69	2.09
$^{166}\text{Hf}$	41.30	20.90	-0.527	1.015	25	77	3.08

with  $R_4 = 2.233$ , and  $^{156}\text{Dy}$  ( $\Delta N = 2$ ) with its value of  $R_4 = 2.932$  is close to the rotor value of 3.3. Table I.2 lists the values of the parameters  $a$ ,  $b$ ,  $c$  as compared with the results in [2]. The value of  $b/a-b$  is  $\sim 0.07$  in  $^{154}\text{Dy}$ , which suggests only a small rotational component ( $\sim 18\%$ ) in the  $2_g$  state. This is in excellent agreement with the value of 20% from the dynamic pairing plus quadrupole (DPPQ) model [2]. Since  $^{156}\text{Dy}$  is a transitional nucleus, the  $a$ ,  $b$ ,  $c$  values show that  $a \neq b$ , i.e.  $E_I$  is not proportional to  $I(I+1)$ . Both terms, the vibrational term  $(a-b)I$  and the softness term  $cI^3$  are required here [2]. In  $^{156}\text{Dy}$ ,  $(a-b)$  is approximately equal to  $b$ , the coefficient of the rotational term. So, there is a considerable rotational component in the

$2_g^+$  state. The shape transition at  $N = 88-90$  with the deformation increasing with  $N$ , is reflected in the drastic increase of the  $[b/a-b]$  value from 0.073 to 1.040, from  $^{154}\text{Dy}_{88}$  to  $^{156}\text{Dy}_{90}$ .

### 3. G-Bands in $^{158-162}\text{Yb}$

The three Yb-isotopes represent one vibrational nucleus  $^{158}\text{Yb}$  with  $R_4 = 2.330$  and two transitional isotopes  $^{160}\text{Yb}$  with  $R_4 = 2.627$  and  $^{162}\text{Yb}$  with  $R_4 = 2.926$ . Table I.3 lists the values of the parameters  $a$ ,  $b$ ,  $c$ . The vibrational structure of the g-band in  $^{158}\text{Yb}$  is reflected in the much larger value of the parameter  $a$  with  $[b/a-b]$  in (2) at only 14%. These values imply only a 30% rotational component in the  $2_g$  state. The shape transition is clearly shown by the decreasing of  $(a-b)$  and, thus increasing of  $[b/a-b]$ . The rotational component in the  $2_g^+$  state increases to 57% (in  $^{160}\text{Yb}_{90}$ ) and to 80% (in  $^{162}\text{Yb}_{92}$ ). A comparison of the obtained values clearly shows the increasing deformation with  $N$ .

### 4. G-Bands in $^{162-166}\text{Hf}$

This part on  $^{162-166}\text{Hf}$  represents an extension of our work on the characterization of aligned bands in even-even Hf isotopes (162, 164, 166, 168) [5]. To our knowledge  $^{162}\text{Hf}$  is the lightest Hf isotope studied so far. It lies far from the line of stability and is only weakly deformed with  $R_4 = 2.561$ . The other two isotopes have  $R_4 = 2.784$  and 2.960 for  $^{164}\text{Hf}$  and  $^{166}\text{Hf}$ , respectively. The three isotopes are transitional isotopes. The rotational contribution of the g-band increases with increasing  $N$  ( $\Delta N = 2$ ), as clearly shown. The values of the parameters are listed in Table I.4. The vibrational contribution, given as  $E_{\text{vib}}\%$ , decreases gradually from 54% for the soft  $^{162}\text{Hf}$  to 25% for the more deformed  $^{166}\text{Hf}$ .

The vibrational and rotational coefficients for the concerned nuclei, discussed here, are summarized in Fig. 1 as functions of the mass number  $A$ . It is apparent that the vibrational coefficient  $(a-b)$  smoothly varies within  $\sim 27$  keV (10%) from one isotone ( $N = 88$ ) to another. The maximum value of 145 keV for Gd ( $Z = 64$ ) then decreases to 118 keV for Er ( $Z = 68$ ) and increases smoothly to  $\sim 126.5$  keV for Yb ( $Z = 70$ ), as shown in Figure 1a. Such a variation explains the light effect of increasing  $Z$  ( $\Delta Z = 2$ ) on the deformation. The shape phase transition at  $N = 88-90$  and the increasing deformation with  $N$  is confirmed by the

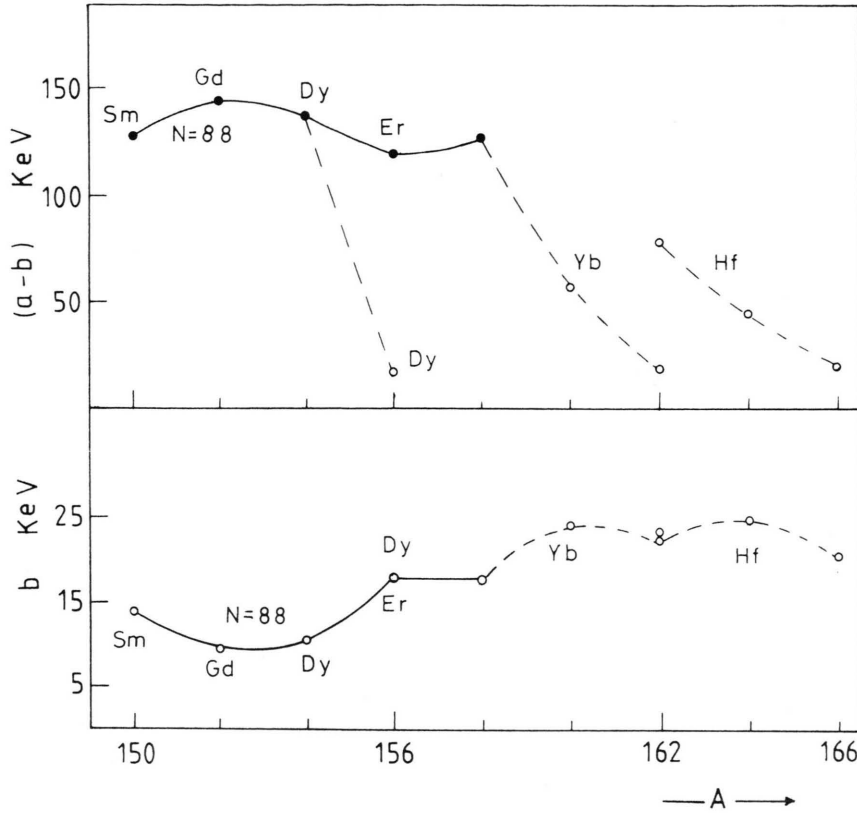


Fig. 1. a) Relation between the vibrational coefficient,  $(a-b)$ , and the mass number  $A$ . b) Relation between the rotational coefficient,  $b$ , and the mass number  $A$ .

shown drastic decreasing from 138.68 keV for the soft  $^{154}\text{Dy}$  to only  $\sim 17$  keV for the transitional  $^{156}\text{Dy}$ . This is also shown for the  $^{158-162}\text{Yb}$  and  $^{162-166}\text{Hf}$  isotopes.

The variation of the rotational coefficient,  $b$ , against the mass number  $A$  is shown in Figure 1 b. The trend of the variation explains the change of the structure from the soft spherical to the more deformed nuclei. It has been found suitable here to give a graphical representation of the vibrational contribution ( $E_{\text{vib}}/E\%$ ) and the rotational contribution ( $E_{\text{rot}}/E\%$ ), each with the angular momentum  $I$ , in Figs. 2 and 3, respectively. Evidently the features of both a spherical vibration and a deformed rotor are present in the same nucleus with different ratios. Table II lists the calculated energies (in keV) of the ground bands of the nuclei  $^{150}\text{Sm} \sim ^{166}\text{Hf}$  as compared with the experimental values.

## II. Systematics of $\mathfrak{I}^{(1)}$ and $\mathfrak{I}^{(2)}$

The gradual phase transition in the range of our study ( $62 \leq Z \leq 72$  and  $88 \leq N \leq 94$ ) may be ex-

plained by examining the systematics of the moments of inertia as functions of spin and position in the shell. The kinematic and dynamic moments of inertia  $\mathfrak{I}^{(1)}$  and  $\mathfrak{I}^{(2)}$ , respectively, are defined [6, 7] as

$$\mathfrak{I}^{(1)} = I / (dE_x / dI) = 2I - 1 / \Delta E_x, \quad (3)$$

$$\mathfrak{I}^{(2)} = I / (d^2 E_x / dI^2) = 4 / (\Delta E_{x1} - \Delta E_{x2}). \quad (4)$$

$\Delta E_{x1}$  and  $\Delta E_{x2}$  are the excitation energy differences between the lowest states with angular momenta  $I$  and ( $I_2$ ) and with ( $I_2$ ) and ( $I_4$ ), respectively.

The variation of the moments of inertia with  $A$  ( $N$  and  $Z$ ) is shown in Fig. 4 for the soft vibrators  $N = 88$  isotones ( $^{62}\text{Sm}$ ,  $^{64}\text{Gd}$ ,  $^{66}\text{Dy}$ ,  $^{68}\text{Er}$  and  $^{70}\text{Yb}$ ) and the transitional isotopes ( $^{156}\text{Dy}$ ,  $^{160,162}\text{Yb}$  and  $^{162,164,166}\text{Hf}$ ). The trend of the moments of inertia  $\mathfrak{I}^{(1)}$  inferred from the  $0^+$  and  $2^+$  states is generally constant with only a 4% variation for  $N = 88$  as  $Z$  varies from 62 up to 70. However, the graph of  $\mathfrak{I}^{(1)}$  inferred from the  $4^+$  and  $6^+$  states shows a partial symmetry about midshell ( $64 \leq Z \leq 66$ ). It is displaced upward by almost a factor of 2.5. Most importantly, the shape transition at  $N = 88-90$  and increas-

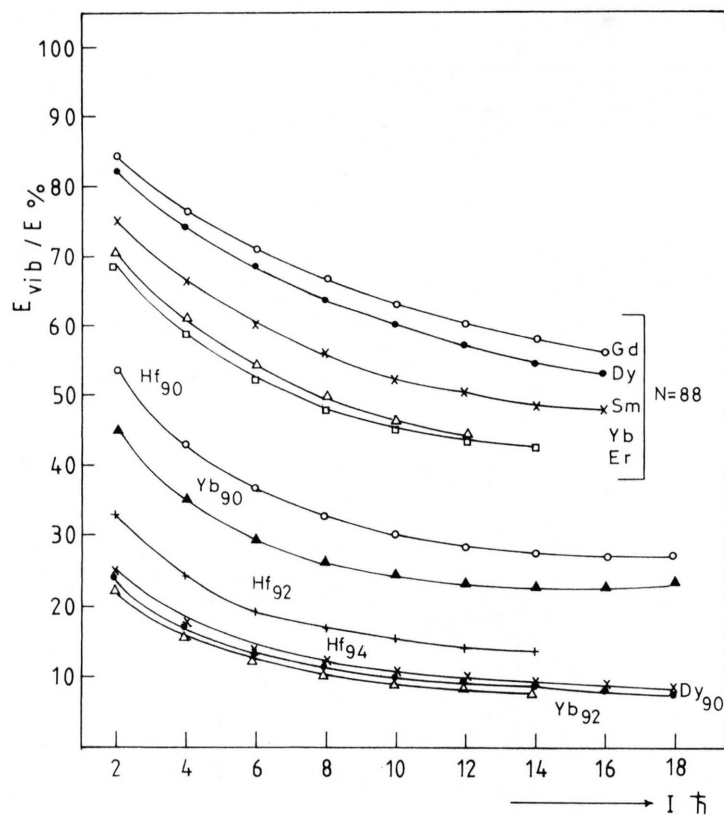


Fig. 2. The vibrational contribution  $E_{\text{vib}}/E\%$  vs. the angular momentum  $I$ .

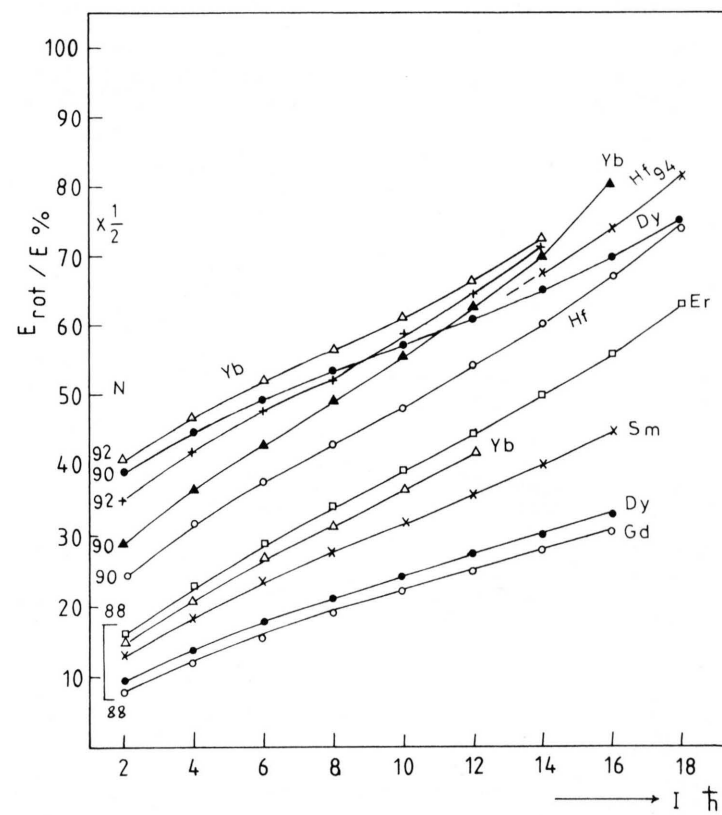
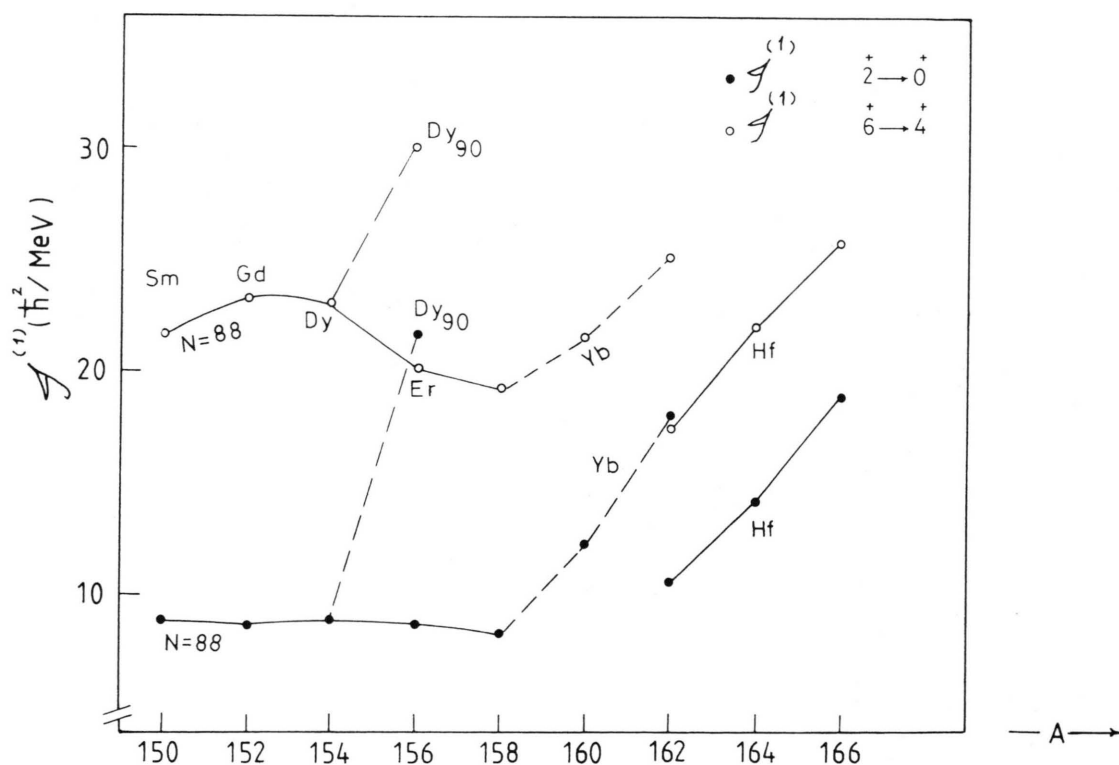


Fig. 3. The rotational contribution  $E_{\text{rot}}/E\%$  vs. the angular momentum  $I$ .

Table II. Experimental and calculated energies (in keV) of the ground bands of the nuclei  $^{150}\text{Sm}$ – $^{166}\text{Hf}$ . The calculated values correspond to the cubic polynomial (2). The values of  $a$ ,  $b$ , and  $c$  are listed in Table I.

Nucleus		$I=2$	4	6	8	10	12	14	16	18
$^{150}\text{Sm}$	Exp.	334	773	1279	1837	2432	3048	3646	4306	
$R_4 = 2.316$	Calc.	337	767	1273	1835	2435	3055	3675	4278	
$^{152}\text{Gd}$	Exp.	344	755	1227	1747	2300	2884	3499	4143	5006
$R_4 = 1.194$	Calc.	345	756	1225	1743	2301	2892	3505	4134	4950
$^{156}\text{Er}$	Exp.	345	797	1340	1959	2633	3315	3837	4381	
$R_4 = 2.2315$	Calc.	342	802	1352	1963	2608	3257	3883	4456	
$^{154}\text{Dy}$	Exp.	335	747	1224	1748	2306	2895	3511	4208	
$R_4 = 2.233$	Cal.	337	745	1216	1741	2308	2910	3537	4179	
$^{156}\text{Dy}$	Exp.	138	404	770	1216	1725	2286	2888	3499	4026
$R_4 = 2.932$	Calc.	138	401	768	1218	1734	2294	2880	3471	4047
$^{158}\text{Yb}$	Exp.	358	835	1404	2048	2745	3429			
$R_4 = 2.330$	Calc.	358	836	1408	2049	2733	3436			
$^{160}\text{Yb}$	Exp.	243	638	1148	1737	2375	2961	3365	3849	4428
$R_4 = 2.627$	Calc.	246	641	1145	1721	2328	2929	3483	3953	4298
$^{162}\text{Yb}$	Exp.	166	487	923	1444	2023	2634	3257		
$R_4 = 2.926$	Calc.	167	484	920	1445	2028	2640	3249		
$^{162}\text{Hf}$	Exp.	285	730	1293	1940	2635	3386	3997	4555	5168
$R_4 = 2.561$	Calc.	189	729	1287	1928	2620	3330	4025	4670	5234
$^{164}\text{Hf}$	Exp.	211	587	1085	1669	2305	2995	3619		
$R_4 = 2.784$	Calc.	212	585	1083	1672	2316	2979	3625		
$^{166}\text{Hf}$	Exp.	158	470	897	1406	1972	2566	3211	3835	4459
$R_4 = 2.960$	Calc.	162	465	885	1396	1973	2591	3223	3845	4432

Fig. 4. The kinematic moments of inertia  $\mathfrak{J}^{(1)}$  as functions of  $A$  values are shown based on the  $2^+ - 0^+$  and  $6^+ - 4^+$  energy differences.

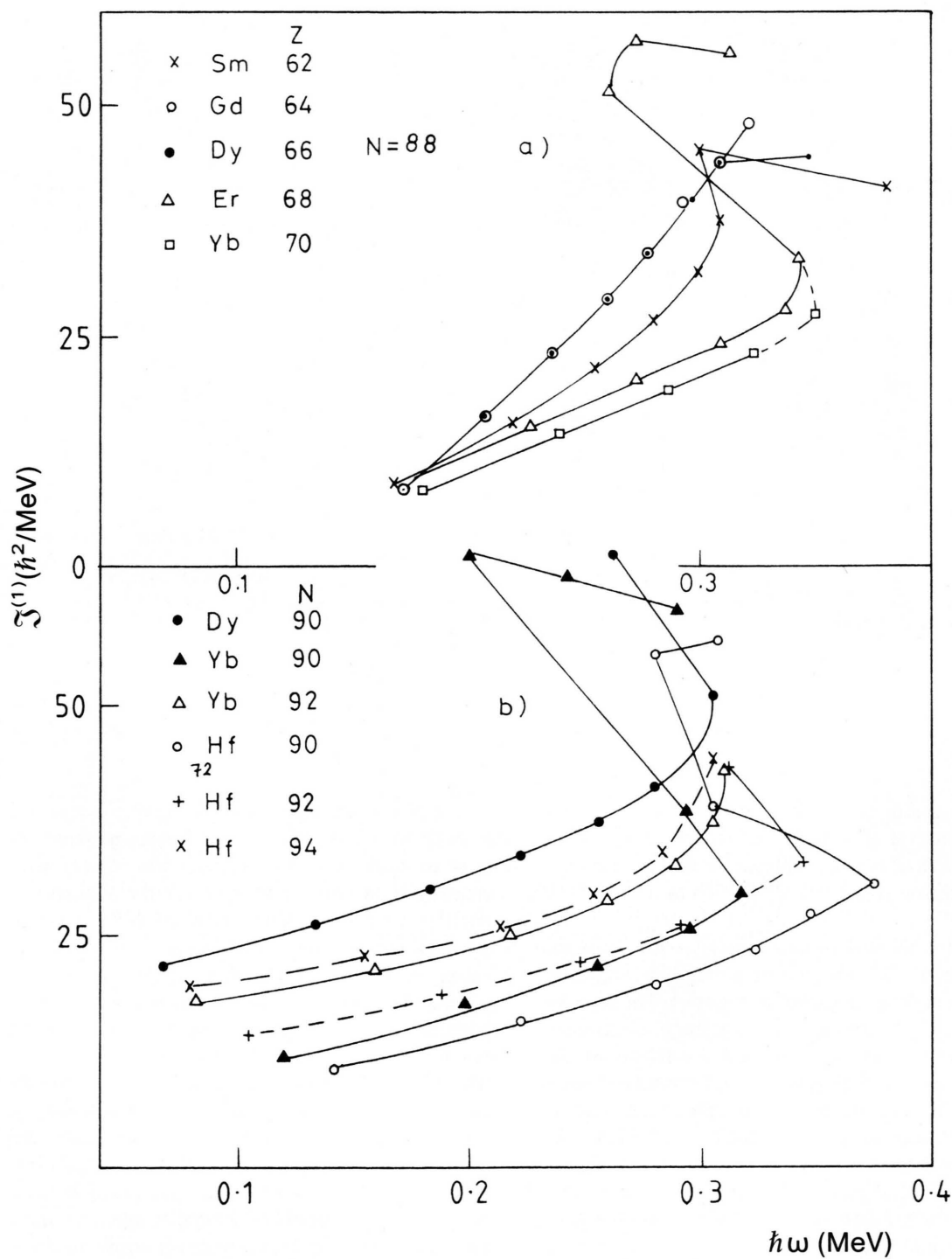


Fig. 5. a) The kinematic moments of inertia  $\mathfrak{J}^{(1)}$  as functions of the rotational frequency  $\omega$  for the  $N=88$  isotones, b) for the transitional nuclei.

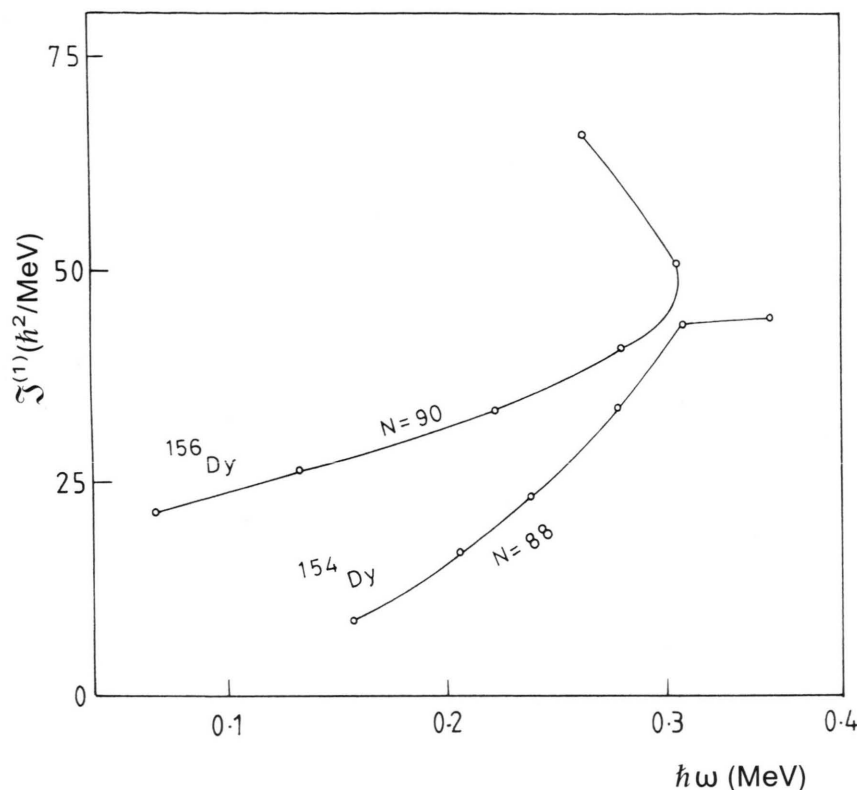


Fig. 6. The kinematic moments of inertia  $\mathfrak{I}^{(1)}$  as functions of the rotational frequency  $\omega$  for  $\text{Dy}_{88}$  and  $\text{Dy}_{90}$  isotopes.

ing deformation with  $N$  is also reflected in the  $\mathfrak{I}^{(1)}$  plots against  $A$  (Figure 4). As stated before, since  $^{154}\text{Dy}$  is soft, it has low  $\mathfrak{I}^{(1)}$  and rises continuously with increasing  $N$  for the  $^{158-162}\text{Yb}$  and  $^{162-166}\text{Hf}$  isotopes.

It is instructive to examine more systematically the dependence of  $\mathfrak{I}^{(1)}$  on spin or rotational frequency. Such a dependence is shown in Figure 5. The increasing trend of  $\mathfrak{I}^{(1)}$  with the rotational frequency is quite evident. The systematics are best illustrated by the behavior of the  $N=88$  isotones and the other transitional nuclei. The moments of inertia of the isotones start from much lower values (below  $9 \hbar^2/\text{MeV}$ ) and increase to 40 to  $45 \hbar^2/\text{MeV}$ , in agreement with Espino and Garrett [8]. Figure 5a, shows a tendency to converge, after some divergence, to the rigid body values at a rotational frequency above  $0.3 \text{ MeV}/\hbar$ . The dependence of  $\mathfrak{I}^{(1)}$  on  $Z$  is also shown. The rate of increase is larger for those at the midshell. Two nuclei  $\text{Gd}$  ( $Z=64$ ) and  $\text{Dy}$  ( $Z=66$ ), which represent the center of the shell, have the same values up to  $\sim 0.3 \text{ MeV}/\hbar$ .

The rate of increase decreases as going below or above the center of the shell. The trend for the moments of inertia to start more but increase less rapidly with increasing  $(\hbar\omega)$  appears to hold for the transitional nuclei (Figure 5b). The starting points shift as a whole to lower values of  $(\hbar\omega)$ . Also, this goes to lower values for lower masses. There is evidence for this trend in the  $\text{Dy}$ ,  $\text{Yb}$  and  $\text{Hf}$  isotopes, and is demonstrated by Fig. 6 for the  $\text{Dy}$  isotopes. The latter figure also shows the shape phase-transition at  $N=88-90$ .

The dynamic moments of inertia  $\mathfrak{I}^{(2)}$  are often compared with kinematic moments  $\mathfrak{I}^{(1)}$  for evidence of rigid rotation. Because of their derivative nature, the dynamic moments accentuate variations in the kinematic moments and tend to vary significantly in these nuclei [3]. The values of  $\mathfrak{I}^{(2)}$  for only some cases have been displayed in Fig. 7 since their variations are often abrupt. It may be concluded that there is a tendency for  $\mathfrak{I}^{(2)}$  to behave as  $\mathfrak{I}^{(1)}$  (up to  $0.3 \text{ MeV}/\hbar$ ) with the rotational frequency and the neutron number  $N$ .



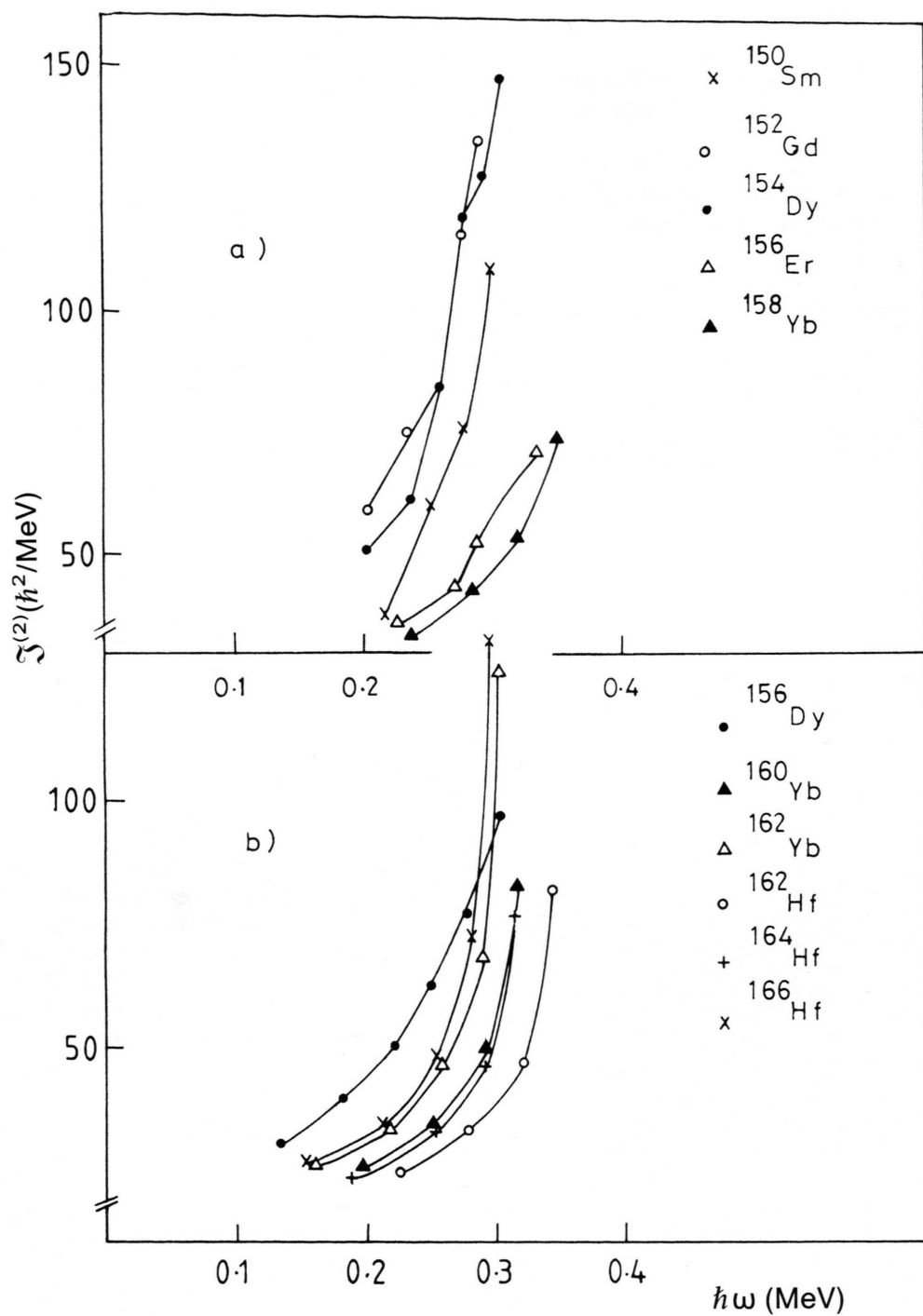


Fig. 7. a) The dynamic moments of inertia  $J^{(2)}$  as functions of  $\omega$  for the  $N = 88$  isotones, b) for the transitional nuclei.



### Conclusion

- (i) The cubic polynomial improves the fit with experimental data for the soft and the weakly deformed nuclei.
- (ii) Based on a systematic analysis of the available data for the concerned nuclei, the vibrational-rotational characteristics have been described.
- (iii) The drastic change at  $N = 88-90$  and some indications of a shape transition are reproduced in our calculations.
- (iv) The gradual changes from the soft  $^{150}\text{Sm}$  to the deformed  $^{166}\text{Hf}$  are reproduced with almost constant parameters and examined by the systematics of the moments of inertia as a function of spin and position.

- [1] T. Tamura, K. J. Weeks, and T. Kishimoto, *Phys. Rev. C* **20**, 3007 (1980).
- [2] J. B. Gupta, *Phys. Rev. C* **39**, 1604 (1989).
- [3] S. L. Tabor, *Phys. Rev. C* **45**, 242 (1992).
- [4] J. B. Gupta, J. H. Hamilton, and A. V. Ramayya, *Nucl. Phys. A* **542**, 429 (1992).
- [5] Egypt-German Springschool and Conference part. and *Nucl. Physics* **2**, 221 (1992). H. E. Abdel-Baeth, Ph.D. thesis, University of Zagazig, Egypt 1993.
- [6] A. Bohr and B. R. Mottelson, *Phys. Scr.* **24**, 71 (1981).
- [7] R. Bengtsson, S. Frauendorf, and F. R. May, *At. Data Nucl. Data tables* **35**, 15 (1986).
- [8] J. M. Espino and J. D. Garrett, *Nucl. Phys. A* **492**, 205 (1989).